

---

# Radiative transfer problem in dusty galaxies: ray-tracing approach

Dmitrij Semionov and Vldas Vansevicius

Institute of Physics, Savanorių 231, LT-03154 Vilnius, Lithuania [dima@itpa.lt](mailto:dima@itpa.lt)

**Summary.** A new code for evaluation of light absorption and scattering by interstellar dust grains is presented. The radiative transfer problem is solved using ray-tracing algorithm in a self-consistent and highly efficient way. The code demonstrates performance and accuracy similar or better than that of previously published results, achieved using Monte-Carlo methods, with accuracy better than  $\sim 3\%$  for most cases. The intended application of the code is spectrophotometric modelling of disk galaxies, however, it can be easily adapted to other cases that require a detailed spatial evaluation of scattering, such as circumstellar disks and shells containing both point and distributed light sources.

## 1 Problem statement

The purpose for the developing radiative transfer problem solving code, described in this article, was to model spatial and spectral energy distribution (SED) observed in external galaxies. The nature of this problem requires ‘self-consistency’ of a solution – the resulting SED of a model must depend only on the SED of stellar sources and assumed properties of dust without any preconditioning on light and attenuation distribution within galaxy [TVA03].

While galaxies in general are complex objects with three-dimensional (3D) distribution of radiation and mater, in most cases they are dominated by axial symmetry (2D), allowing significant simplification of the model geometry. However, the model should account for presence of macroscopic structure within galaxies, possibly including elements having other symmetry, such as bars and spiral arms (2D+).

Most present day astrophysical radiative transfer codes employ either a Monte-Carlo (MC, eg. [CF01]) or a ray-tracing (RTR, eg. [RS99], [RM02]) methods. Some of implementations of these methods were compared by [BD01] for 1D and by [DT02] for 2D cases. The RTR approach allows the optimization of solution for a given system geometry, which was the main reason to use it as a basis for the Galactic Fog Engine (hereafter ‘GFE’), a program for

self-consistent solution of radiative transfer problem in dusty media with primarily axisymmetric geometry. This paper concentrates on radiative transfer in ultraviolet-to-optical wavelength range assuming exclusively coherent scattering, therefore in most equations the wavelength dependence will be omitted.

## 2 Algorithm

### 2.1 Model description

The GFE iteratively solves a discrete bidirectional radiative transfer problem, producing intensity maps of the model under arbitrary inclination at a given wavelength set. The foundation of the iterative evaluation of radiation transfer equation was laid out by Henyey [Hen37]. By solving a set of one-dimensional radiative transfer equations

$$\frac{dI}{ds} = -\kappa I + j + \kappa \frac{\omega}{4\pi} \int I \Phi d\Omega, \quad (1)$$

where  $\Phi$  and  $\omega$  denote the scattering phase function and albedo and  $\kappa$  and  $j$  are absorption and emissivity coefficients of the medium, the initial system SED is separated into: escaped energy, that reaches an external observer; energy, absorbed by grains, that is eventually emitted as thermal radiation; and scattered energy distribution. The solution is then repeated, substituting scattered energy as initial distribution for the next iteration, accumulating resulting escaped and absorbed energy, until certain convergence criteria are met, either a fixed number of iterations, or remaining scattered energy being below specified threshold. After convergence is reached the dust temperature is calculated from absorbed energy distribution. If it is necessary to account for self-scattering of thermal radiation by dust grains, the resulting emission SED can be input into scattering evaluation loop and the process repeated until the final radiative energy distribution is obtained, and then used to produce SED as seen by an external observer.

Calculations are performed within a cylinder with a radius  $r_m$  and height above midplane  $z_m$ , which is subdivided into a set of layers of concentric, internally homogeneous rings ('bins') of arbitrary radial and vertical thickness. Since the linear extent of each individual light source (star) is negligible compared to the size of system, it is possible to solve the radiative transfer problem considering every volume element of the model having both attenuating (light scattering and absorption by interstellar dust) and emitting (light emission by the stars and thermal radiation of the dust particles) properties per unit volume, defining for each ring denoted by indexes  $r$  and  $z$  its total absorption  $k' = \kappa(r, z)$ , and emissivity  $j' = j(r, z, \alpha, \delta)$ , combined from internal light sources and energy scattered within its volume, with angles  $\alpha$  and  $\delta$  defining the direction of radiation propagation.

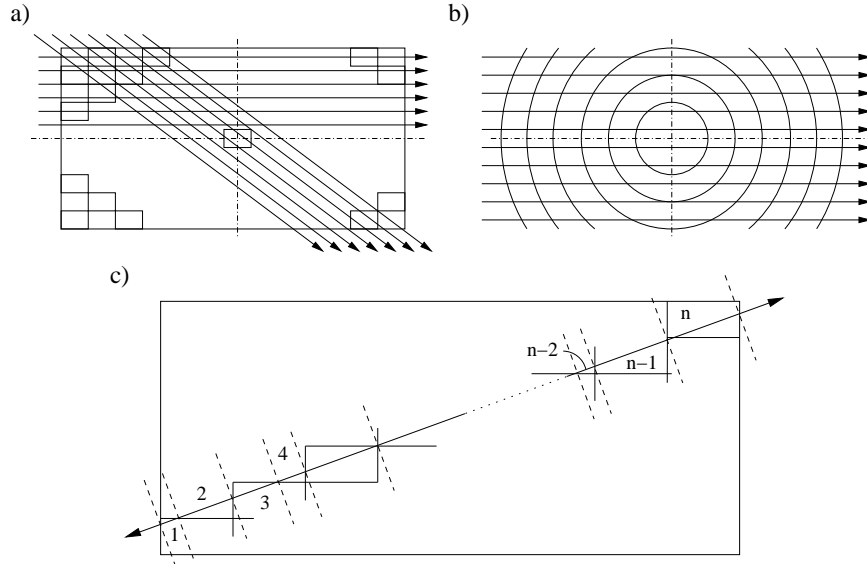


**Fig. 1.** The model geometry. Panel a) shows the diametral, panel b) - central plane cross-section of the model. The distribution and density of ray-tracing paths (shown as arrows) are computed to produce even and sufficient sampling of the model volume. Panel c) illustrates the discrete radiative transfer in cross-section parallel to the model Z axis. Limits of plane-parallel layers for one-directional treatment are shown as dotted lines while boundaries of the individual rings are outlined with solid lines.

## 2.2 Radiative transfer equation

GFE uses static ray-casting geometry, determining the set of rays that ensures a required degree of sampling of the model volume (fig. 1a and 1b). If the viewing solid angle, containing each direction, can be held small, the radiative transfer along these rays can be solved as in plane-parallel homogeneous layer case for a series of intervals traversing rings until crossing the outer boundary of the model (fig. 1c). In a form suitable for computer implementation an incident intensity on a given point for a light path separated into  $n$  intervals of length  $l_i$ , numbered outwards from that point, is written as

$$I_{\text{inc}} = \sum_{i=1}^n \left( \prod_{j=1}^{i-1} e^{-k'_j l_j} \right) \frac{j'_i}{k'_i} (1 - e^{-k'_i l_i}). \quad (2)$$

Similarly, the intensity of radiation scattered with albedo  $\omega$  from a given direction ( $\alpha : \delta$ ) into all other directions within a certain interval denoted by index “1” is

$$I_{1,\alpha,\delta} = \omega j'_1 l_1 - \omega \left(1 - e^{-k'_1 l_1}\right) \left[ \frac{j'_1}{k'_1} - \sum_{i=2}^n \left( \prod_{j=2}^{i-1} e^{-k'_j l_j} \right) \frac{j'_i}{k'_i} \left(1 - e^{-k'_i l_i}\right) \right]. \quad (3)$$

When considering azimuthally inhomogeneous model configuration (3D case), each ring is subdivided into required number of azimuthal segments. The number and directions of rays cast through the system have to be modified accordingly to include new sets of rays in azimuthal direction, however, the ray-tracing part of the algorithm is unchanged. The computational time scales as  $N_{\text{bin}}^{3/2} \times \log N_{\text{bin}}$  for 2D and  $N_{\text{bin}}^{4/3} \times \log N_{\text{bin}}$  for 3D cases.

### 2.3 Scattering phase function

Since angular distribution of radiation at each point in the model is non-isotropic, it must be described using a numerical phase function (matrix), providing the radiation intensity towards a set of predefined reference directions ('RDs') described by angular coordinates ( $\alpha_0 : \delta_0$ ). There exists a number of ways to distribute RDs on a sphere, however, those methods that produce a set of RDs arranged in iso-latitude rows are the most efficient in this particular model geometry, allowing both efficient storage and retrieval of scattered intensity and fast rotation of the phase matrix around model  $Z$ -axis. The memory requirements and the overall algorithm's performance have also to be taken into consideration.

In this work the following methods of RD distribution were compared: HEALPix<sup>1</sup> [GHW99], HTM<sup>2</sup> [KST01], a trivial iso-latitude triangulation (hereafter 'TT', fig. 2a) and a square matrix with elements ('texels') corresponding to evenly spaced ( $\alpha_0 : \delta_0$ ) coordinates (hereafter 'Texel'). For triangulation schemes and HEALPix the radiation intensity towards a given point was interpolated between 3 nearest RDs using either 'flat' (fig. 2b) or 'spherical' (fig. 2c) weights.

## 3 Computational precision

### 3.1 Scattering phase function interpolation

To compare used sphere subdivision and interpolation algorithms a following test model (hereafter a 'standard model') was employed: a cylinder with height to radius ratio  $z_m/r_m = 0.2$ , divided into  $N_{\text{bin}} = 441$  ( $21 \times 21$ ) equally spaced rings, filled with radiating and absorbing particles whose density follows a double exponential law

<sup>1</sup><http://www.eso.org/science/healpix/>

<sup>2</sup><http://www.sdss.jhu.edu/htm/>

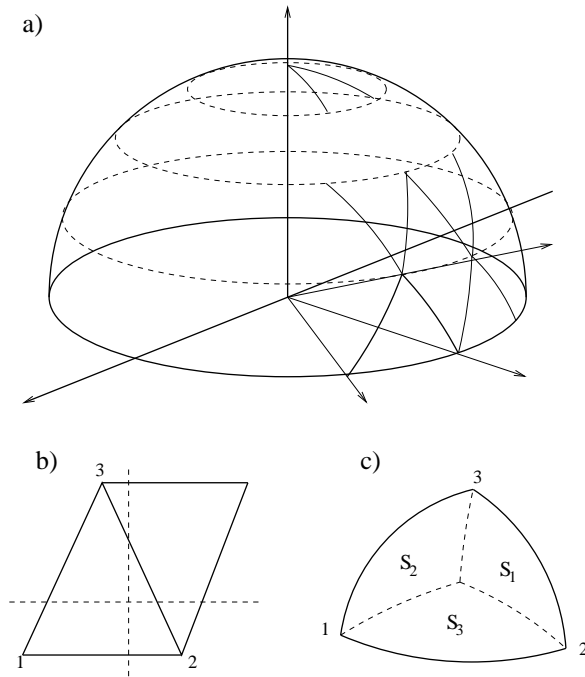


**Fig. 2.** The reference point structure used for interpolation of the scattering phase function. Panel a) shows the trivial iso-latitude triangulation for one hemisphere with reference directions arranged symmetrically against diametral and horizontal planes. Panels b) and c) represent two implemented interpolation schemes, ‘flat’ and ‘spherical’. In case of spherical interpolation, input from each triangle vertex is weighted by the area defined by shortest distances from the given direction to the vertices ( $S_1$  for 1-st vertex and so on).

$$\rho(r, z) = \rho_0 e^{-r/r_0} e^{-z/z_0} \quad (4)$$

with  $r_0 = 0.2r_m$  and  $z_0 = 0.2z_m$  and the model central optical depth perpendicularly to the central plane  $\tau_{ct} = 25$ . The Henyey & Greenstein [HG41] scattering phase function

$$\Phi(\theta) = \frac{1 - g^2}{(1 + g^2 - 2g \cos \theta)^{3/2}} \quad (5)$$

was used with asymmetry parameter  $g = 0.75$ .

The primary quality criteria of a given algorithm is its ability to represent the angular intensity distribution of anisotropic scattering. If the phase function representation is exact, the distribution of values  $(\Phi'(\theta) - \Phi(\theta))/\Phi(\theta)$  (where  $\Phi'(\theta)$  is a resulting numerical phase matrix) would be a  $\delta$ -function. However, since employed methods introduce different types of numerical errors, the actual distribution form depends strongly on the phase function

sampling and the interpolation algorithm. An examples of resulting error distributions (as relative numerical phase matrix deviation from its analytical form) for the algorithms tested are shown on fig. 3.

As can be seen, methods providing uniform sphere coverage produce more preferable error distributions. With the increasing number of RDs the representation of the scattering phase function improves, reducing maximal possible deviation from the true value, particularly for TT (fig. 3a) and HEALPix (fig. 3c) methods, with TT algorithm showing slightly better error distribution form. ‘Spherical’ interpolation scheme (fig. 3, right column in panels a – c) produces more symmetrical error distributions, while ‘flat’ interpolation (left column) in some cases introduces additional numerical errors. When compared with other methods, attempt to reproduce scattering phase function using simple matrix with no interpolation between its elements (Texel scheme, fig. 3d) produces results of average quality, its error distribution quickly reaching a ‘saturated’ form with increasing number of RDs. The described error distribution is somewhat dependent on the orientation of the scattering phase function relative to the set of RDs, this dependence being minimal for the methods with identical size of interpolation elements (HEALPix). All methods that use interpolation display similar performance for a given number of RDs (table 1).

**Table 1.** The normalized computing time for models using different sphere subdivision and scattering phase function interpolation algorithms.

Interpolation method	HEALPix	HTM	TT	Texel
‘flat’	2.5	2.8	2.5	1.0
‘spherical’	8	10	8	–

### 3.2 Volume sampling and subdivision

The problem encountered applying numerical methods is error accumulation. In case of iterative ray-tracing it arises from sampling and interpolation errors. The source of sampling errors is incomplete/inadequate spatial sampling of the system while interpolation errors are related to the scattering phase function approximation, described in the previous section. Both error types independently affect every ray traced through the system, thus the accumulated error increases with the increasing number of bins and rays. This makes oversampling undesirable not only due to increasing computational time, but also for a reason of minimizing numerical errors.

As a measure of method’s quality a defect in energy balance  $E_{\text{err}}$  as a percentage of total energy radiated within system  $E_{\text{tot}}$

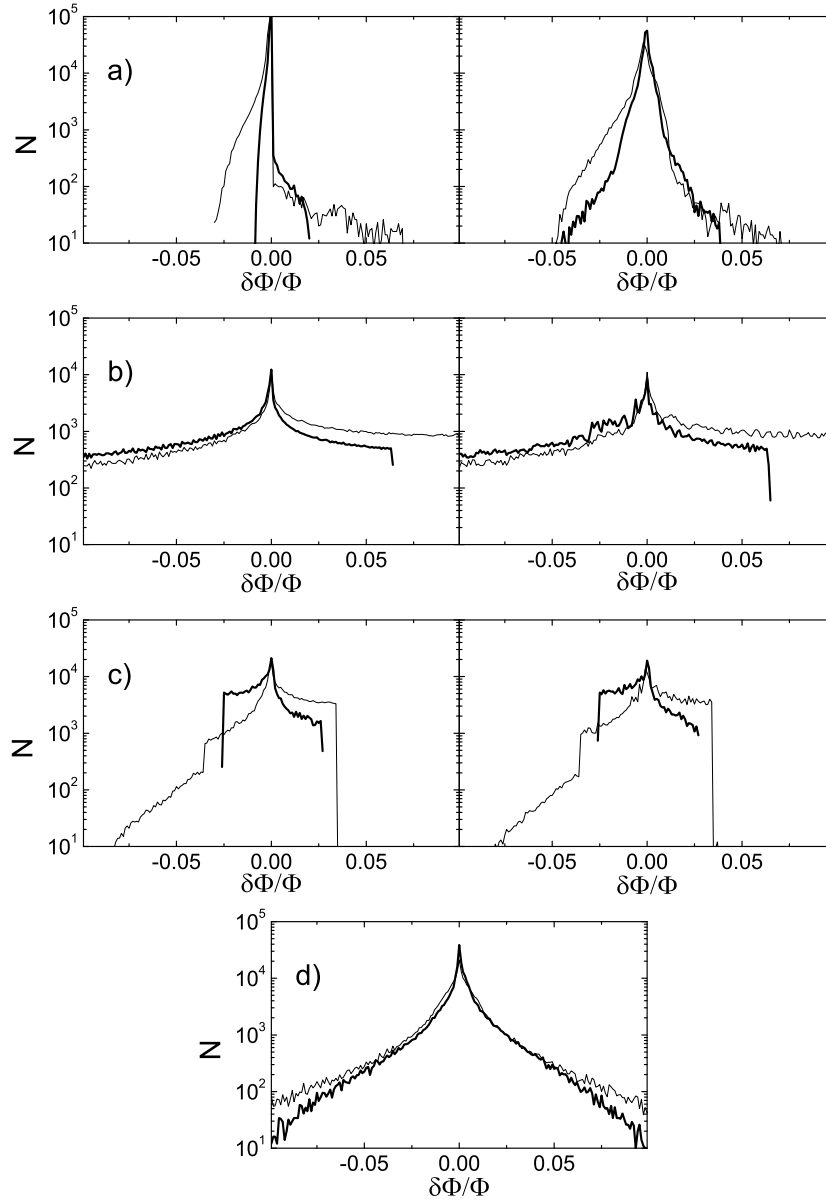


**Fig. 3.** The distribution of relative numerical phase matrix deviation from its analytical form for different sphere subdivision algorithms. Panels a) – d) correspond to TT, HTM, HEALPix and Texel methods. For the first three methods the results obtained using both ‘flat’ (left panels) and ‘spherical’ (right panels) weighted interpolation are presented. Thin line shows the results obtained for approximately 3100, thick line – for approximately 12000 reference directions.

$$E_{\text{err}} = \frac{E_{\text{tot}} - E_{\text{abs}} - E_{\text{sca}} - E_{\text{esc}}}{E_{\text{tot}}} \quad (6)$$

is used. Here  $E_{\text{esc}}$ ,  $E_{\text{abs}}$  and  $E_{\text{sca}}$  are the parts of a total radiated energy that escaped the system, was absorbed and remained to be scattered within the system, respectively.

To determine the sampling and gridding influence on the model precision the following two tests were performed. Firstly, the radiation field in the standard model using TT algorithm with scattering phase function represented by a set of 182 RDs was computed with different number of rays  $N_{\text{ray}}$ , cast through each ring. The results, presented on fig. 4a, show a significant error accumulation effect. Then, keeping a number of rays per ring constant the number of rings  $N_{\text{bin}}$  in model was changed (fig. 4b). As can be seen, improving the sampling of a model decreases the approximation errors to a certain minimum, limited by internal errors of a chosen scattering phase function interpolation method. This geometric configuration can be considered optimal, since with further increase in a number of bins and rays the quality of the solution begins to deteriorate due to error accumulation.

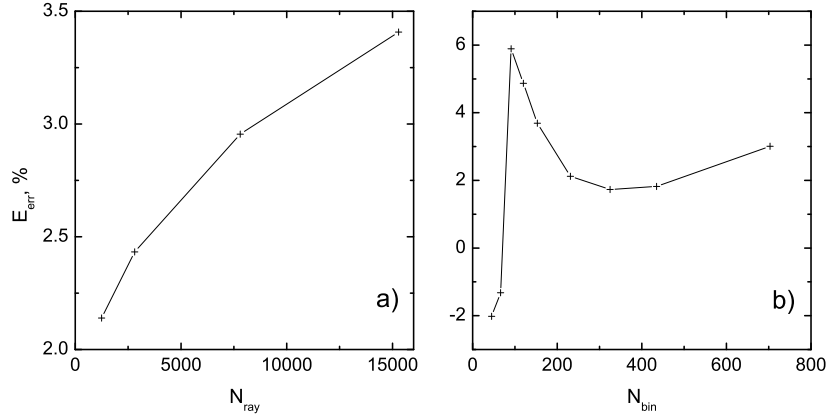


**Fig. 4.** The influence of subdivision and sampling of the model on the energy balance. Panel a) displays the energy defect for a given number of rays cast per model bin; panel b) shows the same quantity for a models consisting of different number of bins.

### 3.3 Dust optical properties

Other important aspect of a numerical radiative transfer solution is its sensitivity to variations in scattering parameters: albedo  $\omega$  and asymmetry parameter  $g$ . Model precision and stability for different  $\omega$  and  $g$  values place



a constraint on the wavelength range where a given method can be applied. The influence of scattering parameters on energy defect was analyzed using the standard model with  $N_{\text{bin}} = 441$  and  $\tau_{\text{ct}} = 10$ .

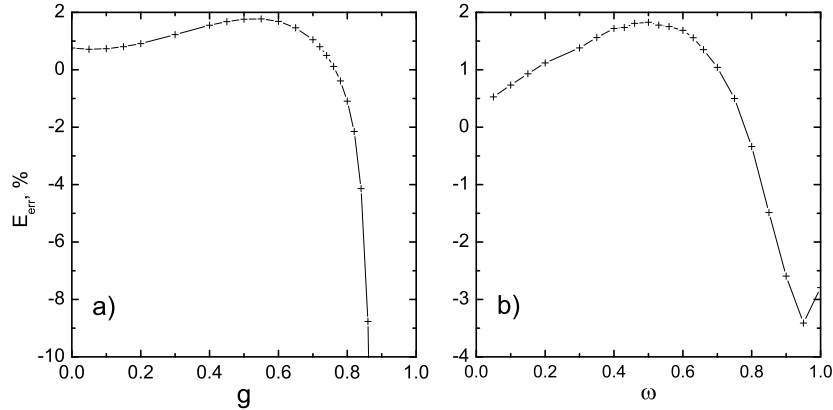


**Fig. 5.** The dependence of the energy losses within model on the grain scattering parameters: scattering phase function asymmetry  $g$  (panel a), with albedo assumed to be  $\omega = 0.5$  for all  $g$  values), and albedo  $\omega$  for  $g = 0.6$  (panel b).

The dependence of overall model precision on scattering asymmetry parameter  $g$  is shown on fig. 5a. The total energy defect after 9 iterations show some variation with the increasing  $g$  up to the limit imposed by the angular scattering phase function gridding (182 RDs) used in the calculations, after which the energy losses in the scattering phase matrix render results invalid.

The effects of the grain albedo on the model accuracy and stability were investigated using similar method. All computations were performed for 7 iterations assuming  $g = 0.6$ . The results are shown in fig. 5b. Within the range of  $\omega$  values, applicable to astrophysical dust grains, those errors stay in acceptable limits, and do not influence the stability of the solution.

## 4 Summary

The code described in this paper has undergone an extensive testing and shows the flexibility and performance satisfying the requirements for the models of the global radiation transfer in dusty galaxies [SV02]. It has been successfully applied to model both integral and position dependent SEDs of several galaxies, some of the first results presented in [SSV03].

The main limiting factor affecting the applicability of the described code is the scattering asymmetry parameter  $g_\lambda$ . In order to correctly treat the scattering with  $g_\lambda$  approaching 1, the number of required reference directions

risers sharply, affecting both the performance and the precision of the method. For a disk galaxy model such as one described in this paper a satisfactory convergence is obtained for  $g_\lambda$  in  $[-0.8 ; 0.8]$  range which includes the optical properties of typical astrophysical grains scattering photons from microwave up to extreme UV wavelengths.

Other model properties, such as optical depth  $\tau_\lambda$  and the relative amount of scattered radiation (dependent on albedo  $\omega_\lambda$ ) seem to have relatively little effect on the quality of the solution. However, models with large optical depth (of order of a few 100's), particularly having a steep matter distribution gradients, require a significant amount of computing time and storage.

The application of this code is not restricted to the systems with dispersed sources and absorbers, the algorithm being easily extended to include treatment of interaction between radiation field and surfaces of macroscopic objects.

*Acknowledgements* This work was supported by a Grant of the Lithuanian State Science and Studies Foundation. Some of the results in this paper have been derived using HEALPix [GHW99] package.

## References

- [BD01] Baes, M., Dejonghe, H.: Radiative transfer in disc galaxies I – A comparison of four methods to solve the transfer equation in plane-parallel geometry. *Mon. Not. Roy. Astron. Soc.*, **326**, 722–732 (2001)
- [CF01] Ciardi, B., Ferrara, A., Marri, S., Raimondo, G.: Cosmological reionization around the first stars: Monte Carlo radiative transfer. *Mon. Not. Roy. Astron. Soc.*, **324**, 381–388 (2001)
- [DT02] Dullemond, C., Turlola, R.: An efficient algorithm for two-dimensional radiative transfer in axisymmetric circumstellar envelopes and disks. *Astron. Astrophys.*, **360**, 1187–1202 (2000)
- [GHW99] Górski, K., Hivon, E., Wandelt, B.: Analysis Issues for Large CMB Data Sets. In: Banday, A., Sheth, R., Da Costa, L. (eds.) *Proceedings of the MPA/ESO Cosmology Conference "Evolution of Large-Scale Structure"*. PrintPartners Ipskamp, NL, 37–42 (1999)
- [Hen37] Henyey, L.: The illumination of reflection nebulae. *Astrophys. J.*, **85**, 107–138 (1937)
- [HG41] Henyey, L., Greenstein, J.: Diffuse radiation in the Galaxy. *Astrophys. J.*, **93**, 70–83 (1941)
- [KST01] Kunszt, P., Szalay, A., Thakar, A.: The Hierarchical Triangular Mesh. In: Banday, A., Zaroubi, S., Bartelmann, M. (eds.) *Mining the Sky: Proc. of the MPA/ESO/MPE workshop, Garching*. Springer-Verlag Berlin Heidelberg, 631–637 (2001).
- [RS99] Razoumov, A., Scott, D.: Three-dimensional numerical cosmological radiative transfer in an inhomogeneous medium. *Mon. Not. Roy. Astron. Soc.*, **309**, 287–298 (1999)
- [RM02] Razoumov, A., Michael, M., Abel, T., Scott, D.: Cosmological Hydrogen Reionization with Three-dimensional Radiative Transfer. *Astrophys. J.*, **572**, 695–704 (2002)

- [SV02] Semionov, D., Vasevičius, V.: Radiative transfer problem in dusty galaxies: ray-tracing vs. Monte-Carlo. *Balt. Astron.* **11**, 537–545 (2002)
- [SSV03] Semionov, D., Stonkutė, R., Vasevičius, V.: Modelling the radial color profile of M31. *Balt. Astron.* **12**, 633–636 (2003)
- [TVA03] Takagi, T., Vasevičius, V., Arimoto, N.: Spectral Energy Distributions of Dusty Galaxies. *Publications of the Astronomical Society of Japan*, **55**, 385–407 (2003)